Tunable Microwave Resonators Using Magnetostatic Wave in YIG Films

WAGUIH S. ISHAK, MEMBER, IEEE, AND KOK-WAI CHANG, MEMBER, IEEE

Abstract—**The purpose of this paper is to review the status of magnetostatic wave (MSW) resonators and to describe, in detail, the theory of operation of the recently developed straight-edge resonators. These resonators are based on magnetostatic waves propagating in high Q cavities fabricated in thin ferrimagnetic films. The resonance frequency of these resonators can be tuned via a bias magnetic field. The theory of propagation of magnetostatic wave devices in periodic arrays will be briefly described followed by a detailed overview of the different configurations for MSW resonators. Three distinct classes of resonators will be discussed: 1) resonators based on array reflectors (deposited metals and etched grooves) will be described in detail; 2) guided-wave ring resonators will be discussed; and 3) the theory of operation and design criteria for the straight-edge resonators will be described. Each class will be evaluated, pointing out the advantages and drawbacks, and whenever applicable, the power handling properties and the phase noise performance will be given.**

NOMENCLATURE

a	Width of microstrip transducer (μm).
d	Thickness of YIG film (μm).
d_1	Thickness of ungrooved YIG film (μm).
d_2	Thickness of grooved YIG film (μm).
g	Normal separation between YIG film and transducer (μm).
H	Bias magnetic field (Oe).
k	Wavenumber of magnetostatic wave (rad/m).
k_1	Wavenumber of ungrooved YIG film (rad/m).
k_2	Wavenumber of grooved YIG film (rad/m).
k_n^+	Wavenumber of main resonance (n) on top surface of YIG film (rad/m).
k_n^-	Wavenumber of main resonance (n) on bottom surface of YIG film (rad/m).
$k_{n,m}$	Wavenumber of width mode (m) inside the YIG film (rad/m).
$k_{n,m}^+$	Wavenumber of width mode (m) on top surface of YIG film (rad/m).
$k_{n,m}^-$	Wavenumber of width mode (m) on bottom surface of YIG film (rad/m).
l	Length of rectangular YIG film along the propagation direction (μm).
ℓ	Equivalent length of the resonator cavity (μm).
L_{trans}	Length of the microstrip transducer (μm).
$\boldsymbol{n}$	Vector normal to the YIG film plane.
n	Main mode number.
N	Number of grooves in the reflecting grating.
m	Width mode number.
Q_{ext}	Q associated with circuits connected to microstrip transducer.
Q_m	Q associated with YIG film losses (material Q).
Q_r	Q associated with leakage through imperfect reflecting gratings.
R	Reflection coefficient of the reflective grating.
s	Lateral separation between YIG film and microstrip transducer (μm).
S	Separation between YIG film and second ground plane (μm).
t	Separation between YIG film and first ground plane (μm).
T	Transmission coefficient of reflective grating.
W	Width of YIG film normal to propagation direction (μm).
Z_1	Wave impedance of ungrooved YIG film (Ω).
Z_2	Wave impedance of grooved YIG film (Ω).
Z_r	Ratio between Z_1 and Z_2.
α	Loss factor (loss(dB) $= -10\log(\alpha)$).
γ	Gyromagnetic ratio (2.8 MHz/Oe).
ΔH	Ferrimagnetic linewidth (Oe).
ΔH_K	Spinwave linewidth (Oe).
λ_0	MSW wavelength (μm).
λ_{em}	Electromagnetic wavelength (μm).
μ_0	Permeability of free space ($= 4\pi \cdot 10^{-7}$ H/m).
τ	Group delay of MSW (μs).
τ_r	Group delay associated with MSW propagating around the ring resonator (μs).
ω	$2\pi\gamma H$ = frequency of MSW (MHz).
ω_M	$2\pi\gamma(4\pi M_s)$, frequency associated with saturation magnetization (MHz).
$4\pi M_s$	Saturation magnetization of YIG film (Gauss, G).

Manuscript received March 28, 1986; revised June 2, 1986.

The authors are with Hewlett-Packard Laboratories, Palo Alto, CA 94304.

IEEE Log Number 8610554.

I. INTRODUCTION

MAGNETOSTATIC WAVES propagating in liquid-phase epitaxially grown yttrium iron garnet films (LPE-YIG) provide a convenient means for performing signal processing functions directly at microwave frequencies. Among the components that can be built using magnetostatic wave (MSW) propagation in YIG films are delay lines, filters, resonators, convolvers, and correlators. The interested reader is referred to [1]–[4] for a review of the subject.

Planar MSW resonators are among the MSW components with potential applications in instruments and communication systems. These tunable resonators can be used

0018-9480/86/1200-1383$01.00 ©1986 IEEE

as the frequency selective elements in tunable oscillator circuits in the 0.5–26-GHz frequency range. The planar structure of the resonator makes integration with MMIC devices easy and attractive. Moreover, because the velocity of propagation of magnetostatic waves in YIG films is only two orders of magnitude lower than the velocity of light, the linewidths involved in fabricating MSW resonators are of the order of 10–100 μm, allowing straightforward photolithographic processing.

In 1976, Skyes *et al.* [5] were the first to give the theory of magnetostatic surface wave (MSSW) propagation in periodic structures using selectively etched grooves in YIG films. They showed good agreement between theory and experiments in the 2–4-GHz frequency range using 9-μm films and 1-μm-deep grooves. Parekh *et al.* [6] reported on the reflection of magnetostatic forward volume waves (MSFVW) by a shallow grooved grating on a YIG film. Their theoretical treatment employed the field theory in conjunction with the theory of two-mode coupling. In 1977, Collins *et al.* [7] reported on the use of etched grooves in YIG films to build one-port tunable resonators and in 1978, Owens *et al.* [8] extended the idea to two-port resonators. These resonators were fabricated using a flip-over configuration in which the coupling transducers were deposited on dielectric substrates and then brought into contact with a YIG film in which two sets of reflecting arrays were etched. At *S*-band, the resonator insertion loss was about 12 dB and the measured Q was about 850. The resonators reported in [5]–[8] used MSSW's in which the bias magnetic field was applied in the plane of the YIG film and normal to the direction of wave propagation. Castera [9] reported on a two-port resonator configuration using MSFVW's and obtained an insertion loss of 12 dB and a loaded Q of 550.

In 1980, Brinlee *et al.* [10] extended the idea of one-port and two-port etched groove resonators to resonators using metal reflective arrays. Their motivation was the difficulty of etching accurate grooves in YIG. Because of the excessive eddy current loss in these metal arrays, the insertion loss of the resonators they fabricated was more than 30 dB and the loaded Q was 600. A novel resonator configuration using MSSW's in a two-cavity structure was reported by Castera *et al.* [11]. The first cavity was long and supported several modes with high Q and the second cavity was short and supported only a single mode. The first cavity set the resonator Q and the second cavity selectively filtered out a single mode. An insertion loss of 15 dB was obtained with a loaded Q of 500 in the 2–4-GHz frequency range. The main disadvantage of this scheme was the device length, which necessitated a large magnet to bias the device. A MSFVW multipole resonator was reported in 1982 by Castera *et al.* [12] in which two resonators were coupled together through a grating placed 45° from both resonators. This grating resulted in good off-resonance rejection of more than 15 dB. The resonator insertion loss was 22 dB at 3 GHz and the loaded Q was 500.

In 1984, Poston *et al.* [13] reported on a new microwave resonator based on guided magnetostatic surface waves.

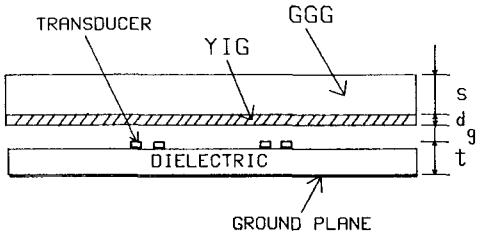

Fig. 1. A typical MSW delay line configuration.

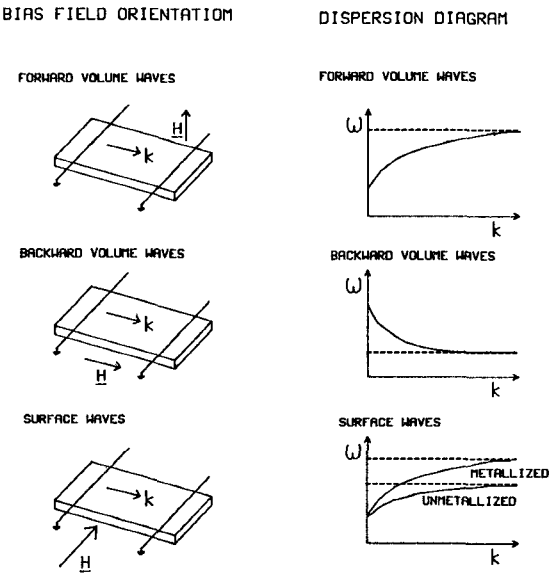

Fig. 2. Dispersion relations for MSFVW's, MSBVW's, and MSSW's.

The waves were guided around a closed circular path using nonuniform in-plane fields. This multiresonant structure exhibited an insertion loss of about 12 dB and loaded Q's as high as 1100.

In the same year, Huijer *et al.* [14] reported on a novel resonator configuration in which a rectangular piece of YIG film was used to reflect the magnetostatic waves at the straight edges of the film. The device was tuned in the 3–9-GHz frequency range using MSSW's and exhibited an insertion loss of 22 dB with Q's from 900 to 4000 [15]. Motivated by the higher Q and the simplicity of the design, Chang *et al.* [16] optimized the straight-edge resonators (SER's) and obtained a tunable device in the 2–16-GHz range with less than 8 dB of insertion loss using MSSW's. Recently, the idea was extended to volume wave resonators with a tuning range of 1–22 GHz and with an insertion loss of less than 10 dB [17].

It is the purpose of this paper to review the different configurations of MSW resonators and to describe the advantages and disadvantages of each, with emphasis on design criteria and practical applications. First, the theory of MSW propagation in ferrimagnetic films will be reviewed, followed by a review of grating-based resonators including one-port and two-port structures. The ring resonator will be described next and finally, the straight-edge resonator will be described in detail. Whenever applicable, the temperature performance, power-handling characteristics, and phase noise data will be given.

II. MSW Modes of Propagation

The propagation of MSW's in ferrite slabs has been treated by Damon and Eshbach [18], who considered three distinct orientations of the bias magnetic field $\boldsymbol{H}$ with respect to the wave vector $\boldsymbol{k}$. In terms of a unit vector normal to the ferrite slab $\boldsymbol{n}$, the three modes of propagation are: 1) magnetostatic forward volume waves, MSFVW: $\boldsymbol{H}\times\boldsymbol{n}=0$; 2) magnetostatic surface waves, MSSW: $(\boldsymbol{H}\times\boldsymbol{n})//\boldsymbol{k}$; 3) magnetostatic backward volume waves, MSBVW: $\boldsymbol{H}//\boldsymbol{k}$.

The dispersion relations for the three MSW modes were given by Daniel *et al.* [19] and will be reproduced below for convenience (see Fig. 1).

A. MSFVW Dispersion Relation

$$\tan(\eta k_1 d)=\eta\cdot\frac{\tanh(k_1 t)+\tanh(k_1 S)}{\eta^2-\tanh(k_1 t)\cdot\tanh(k_1 S)} \tag{1}$$

where

$$k_1^2=(\pi/W)^2+k^2 \tag{2}$$

$$\eta^2=\frac{4\pi M_s H}{(\omega/\gamma)^2}-1. \tag{3}$$

B. MSBVW Dispersion Relation

$$e^{2A_1 d}=\frac{[\mu_1 A_1-\mu_2 k_z-B_1\cdot\tanh(B_1 S)]\cdot[\mu_1 A_1+\mu_2 k_z-B_1\cdot\tanh(B_1 t)]}{[\mu_1 A_1+\mu_2 k_z+B_1\cdot\tanh(B_1 S)]\cdot[\mu_1 A_1-\mu_2 k_z+B_1\cdot\tanh(B_1 t)]} \tag{4}$$

where

$$\mu_1^2=-\eta^2 \tag{5}$$

$$\mu_2=\frac{4\pi M_s(\omega/\gamma)}{(\omega/\gamma)^2-H^2} \tag{6}$$

$$A_1^2=(k^2/\mu_1)+k_z^2 \tag{7}$$

$$B_1^2=k_z^2+k^2 \tag{8}$$

$$k_z=\pi/W. \tag{9}$$

C. MSSW Dispersion Relation

$$e^{2A_2 d}=\frac{[\mu_1 A_2-\mu_2 k-B_2\cdot\tanh(B_2 S)]\cdot[\mu_1 A_2+\mu_2 k-B_2\cdot\tanh(B_2 t)]}{[\mu_1 A_2+\mu_2 k+B_2\cdot\tanh(B_2 S)]\cdot[\mu_1 A_2-\mu_2 k+B_2\cdot\tanh(B_2 t)]} \tag{10}$$

where

$$A_2^2=\frac{(\pi/W)^2}{\mu_1}+k^2 \tag{11}$$

$$B_2^2=(\pi/W)^2+k^2. \tag{12}$$

Fig. 2 shows the dispersion relations for the three modes plotted versus the wavenumber k.

D. MSW Propagation in Periodic Structures

Because magnetostatic waves can be considered as a TE mode propagating in waveguides, a periodic structure in YIG films can be analyzed using standard theories for cascaded transmission lines. Fig. 3 shows a schematic of a cross section for a periodic array formed by etching grooves on the top surface of the YIG film. It can be shown that [5] the ratio of wave impedances between the ungrooved (thickness $=S_1$) and the grooved (thickness $=S_2$) regions is given by

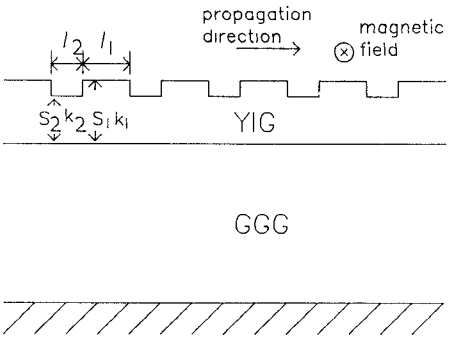

Fig. 3. Etched grooves in YIG films (after Skyes *et al.* [5]).

$$Z_r=Z_1/Z_2=k_2/k_1=S_1/S_2. \tag{13}$$

The amplitude reflection and transmission coefficients are related to the number of grooves in the grating N by the relations

$$|R|=\frac{Z_r^{2N}-1}{Z_r^{2N}+1} \tag{14}$$

$$|T|=\frac{2Z_r^N}{Z_r^{2N}+1}. \tag{15}$$

The loaded Q of the resonator is computed as follows [8]:

$$\frac{1}{Q_l}=\frac{1}{Q_r}+\frac{1}{Q_m}+\frac{1}{Q_{\text{ext}}} \tag{16}$$

where Q_r, Q_m, and Q_{ext} are the quality factors associated with leakage through imperfectly reflective gratings, YIG film propagation losses, and external loading circuits, respectively. The expressions for Q's follow:

$$Q_r=\frac{2\pi\ell}{\lambda_0(1-R^4)} \tag{17}$$

$$Q_m=\frac{\omega\tau}{2\alpha} \tag{18}$$

where ℓ, λ_0, and τ are the effective cavity length, wavelength, and group delay, respectively. The loss factor α is related to the propagation loss by: loss(dB) $=-10\log(\alpha)$,

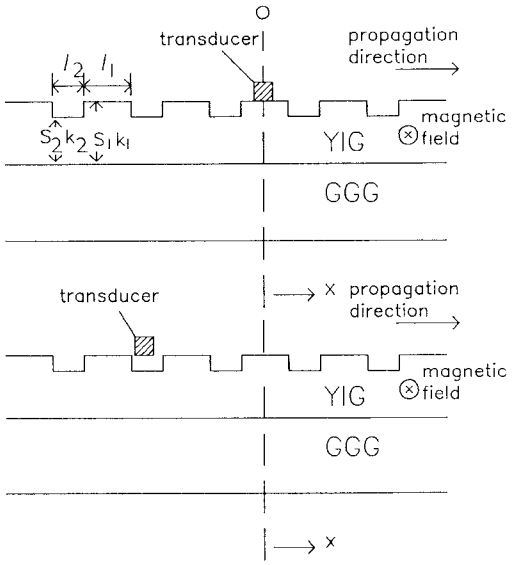

Fig. 4. One-port, etched-groove resonators (after Collins *et al.* [7]).

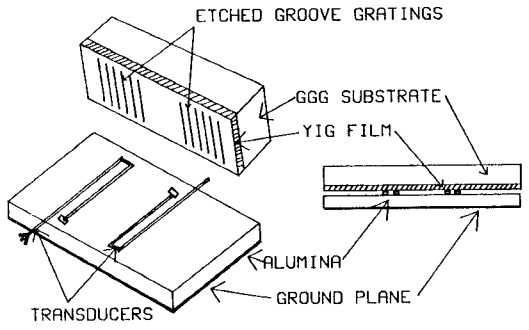

Fig. 5. Two-port, etched-groove resonators (after Owens *et al.* [8]).

where α is a function of the material linewidth. Notice that Q_m is directly proportional to the resonance frequency ω. Therefore, MSW resonators should exhibit higher loaded Q's at higher tuning frequencies. This has been verified experimentally [16].

III. Grating-Based MSW Resonators

A. MSSW Resonators

The first MSW resonator reported [7] was a one-port, MSSW resonator structure employing a microstrip transducer in the vicinity of a uniform periodic array of etched grooves (Fig. 4). The grooves, 38 in number, were 30 μm wide and 4000 μm long each and were separated by 120 μm. They were etched to a depth of 1 μm in a 9-μm YIG film. In their 1978 paper [8], Owens *et al.* reported on a two-port MSSW resonator (Fig. 5) as an extension of the one-port resonator mentioned previously. They gave a theoretical model to predict the insertion loss of the resonator and the agreement between theory and experiment at 3 GHz was impressive. When the microstrip transducers were closely coupled to the YIG film, the resonator's insertion loss was about 13 dB, the loaded Q was 775, and the off-resonance rejection was only 8 dB. Adding a decoupling layer of 35 μm between the transducers and the YIG film resulted in a better off-resonance rejection, about 10 dB, and the overall spurious suppression was more than 15 dB.

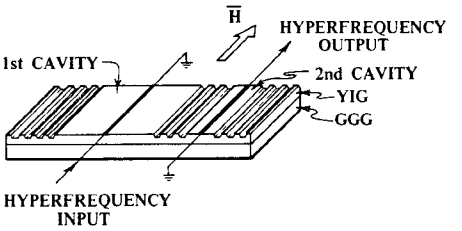

Fig. 6. Two-cavity MSSW resonators (after Castera [11]).

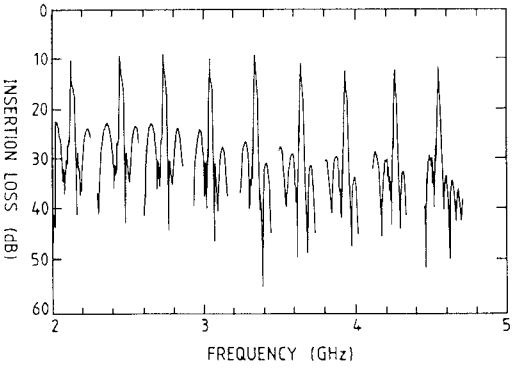

Fig. 7. Tuning characteristics of two-cavity resonators (after Castera [1]).

One-port and two-port resonators using metal arrays as reflective gratings were fabricated and tested by Brinlee *et al.* [10]. These resonators are simple to build since they do not require etching grooves in the YIG film. A thin aluminum film was first sputtered on YIG and then the gratings were defined photolithographically and chemically etched. Because of the eddy currents induced in the metal films, the insertion loss of the two-port device was as high as 32 dB with an off-resonance isolation of only 4 dB. The authors gave a theoretical model explaining the frequency response of the device and the agreement between theory and experiment was good.

To obtain a better off-resonance suppression, Castera *et al.* [12] fabricated a two-cavity MSSW resonator as shown in Fig. 6. The first cavity was a long one with two high-reflection etched-groove arrays. This cavity supported several high Q resonance modes. The second cavity was short and monomode with a lower Q value and was used to filter one mode from the first cavity. Fig. 7 shows the tuning characteristics of this resonator in the 2–5-GHz frequency range. The loaded Q was 500 and the off-resonance rejection was 15 dB. The resonator exhibited a negative temperature coefficient, common to all MSSW devices, and was measured to be -1375 ppm/°C at 3 GHz and -376 ppm/°C at 13 GHz.

Although MSSW resonators exhibit low insertion loss and relatively high Q, they suffer from two main drawbacks.

1) Because the bias magnetic field is applied in the plane of the film, a large magnet gap is required, resulting in a large overall magnet as well as a large power dissipa-

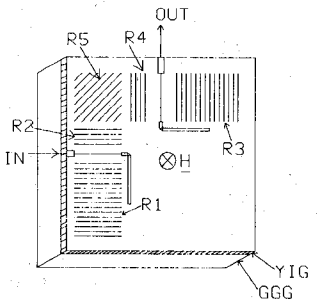

Fig. 8. Two-cavity MSFVW resonators (after Castera *et al.* [12]).

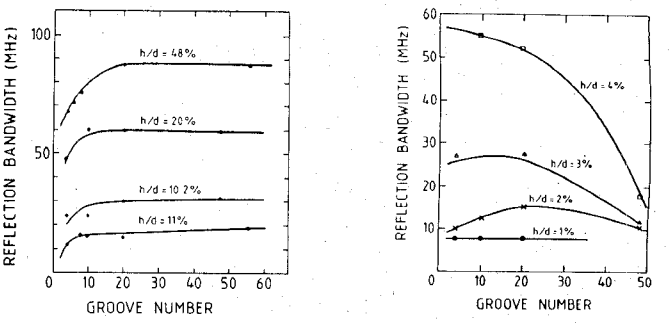

Fig. 9. Effect of number of grooves on reflection bandwidths for (a) MSSW resonators and (b) MSFVW resonators (after Castera [1]).

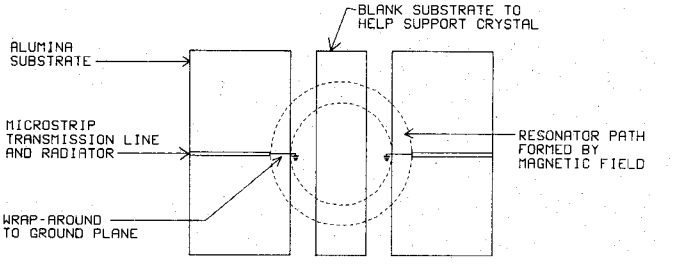

Fig. 10. MSSW ring resonators (after Poston *et al.* [13]).

tion in the magnet coil. This is especially true for the two-cavity resonator, which typically measures 10×5 mm. This resonator would require an electromagnet with a gap dimension of about 20×6 mm.

2) The coincidence limiting phenomenon, which is due to first-order nonlinear effects in ferrite films, occurs at frequencies up to 4 GHz with MSSW devices. The result is saturation at -10 dBm below 4 GHz.

B. MSFVW Resonators

Because MSFVW transducers are bidirectional, any of the above MSSW resonator structures would give a poor off-resonance isolation if used in the volume wave configuration. To avoid this drawback, Castera *et al.* [9] came up with a new configuration involving two magnetically coupled cavities. Each cavity consisted of two etched-groove gratings and a single microstrip transducer. The two cavities were placed at a 90° angle and were coupled by a 45° oblique incidence reflective track changing grating, as shown in Fig. 8. The authors reported on the relation between the reflection bandwidth of the attenuation notch versus the number of grooves in ion-milled gratings with the relative groove depth (depth/width ratio) as a parameter. They showed that MSFVW's were reflected more easily than MSSW's. For example, using 20 grooves, a notch depth of 30 dB was reached with a relative groove depth of 21 percent for MSSW's and 4.2 percent for MSFVW's. Fig. 9 is a graph taken from [2] to demonstrate this comparison. The best results were obtained at a wavelength of 150 μm using single microstrip transducers 20 μm wide and 3 mm long. The relative groove depth was 1.5 percent. The numbers of grooves used were: 50, 10, and 10 for gratings (R1, R3), (R2, R4), and R5, respectively. The resonators exhibited an insertion loss of between 20 and 32 dB and a loaded Q value of 290 to 1570 over a tuning range of 2–11 GHz. In contrast to the MSSW case, these MSFVW resonators exhibited temperature coefficients of $+3280$ ppm/°C at 3 GHz and $+740$ ppm/°C at 13 GHz. These positive coefficients can be balanced by the negative coefficient of commercially available permanent magnet materials, as demonstrated previously by Adam *et al.* [20]. While this is an advantage of MSFVW devices, the permanent magnet compensation will be exact at only one frequency with large deviations occurring at other frequencies within the tuning range. As an illustration, and using the above-mentioned temperature coefficients, the above resonator requires bias field values of 2831 G at 3 GHz and 6402 G at 13 GHz for a YIG film with 1760-G saturation magnetization. The shift in the resonator frequency will be 9.84 MHz/°C at 3 and 13 GHz. These shifts correspond to a change of 3.5 Oe in the bias magnetic field. The bias magnet should provide an opposite shift in the magnetic field of 3.5 Oe at both frequencies. In terms of ratios of the bias field values, these shifts correspond to -0.124 percent (3.5/2831) and -0.055 percent (3.5/6402) at 3 GHz and 13 GHz, respectively. Therefore, in order to achieve exact compensation over the entire tuning range, a magnet with a variable temperature coefficient of remanence is required.

Two more effective methods of temperature compensation can be used.

1) The YIG film can be ovenized and held at an elevated temperature [21] in the same manner as YIG spheres are heated. The main disadvantage is the extra power required for the heater.

2) The YIG temperature can be sensed and feedback circuitry used to change the current input to the bias electromagnet to compensate for the temperature change [22]. This method requires simple circuitry and has the potential of exact compensation over wide frequency ranges.

IV. Ring Resonators

Fig. 10 shows a schematic of a guided-wave ring resonator using MSSW's propagating around a circular path in thin YIG films [13]. The bias field was supplied by a permanent magnet with concentric north and south poles. Two diametrically opposite microstrip transducers were used to couple energy in and out of the resonator. The frequency response of the resonator was tuned between 2

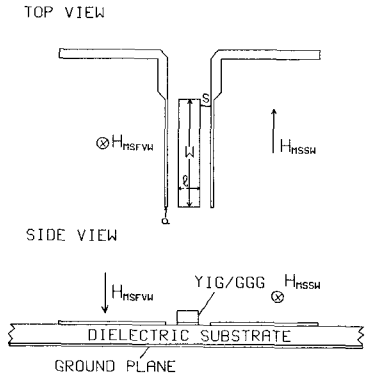

Fig. 11. Straight-edge resonators (after Huijer *et al.* [14]).

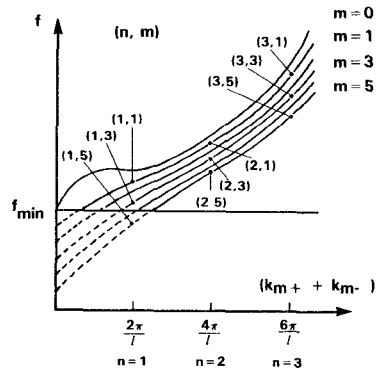

Fig. 12. Dispersion characteristics of MSSW width modes.

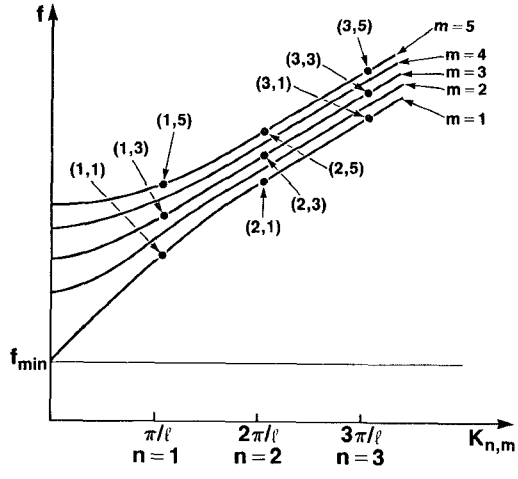

Fig. 13. Dispersion characteristics of MSFVW width modes.

and 4 GHz by mechanically adjusting the gap. The resonator frequency response was multiresonant with frequency separation determined by

$$\Delta\omega = v_g \cdot \Delta k \tag{19}$$

where Δk is the change in the wavenumber between resonances. Substituting $1/\tau_r$ for v_g, (19) reduces to

$$\Delta f = 1/\tau_r \tag{20}$$

where τ_r is the group delay for propagation around the ring. Using a 19-μm-thick YIG film, the separation between resonances was about 10 MHz at a center frequency of 2 GHz. The loaded Q varied between 1100 and 1900 and the insertion loss was between 12 and 26 dB, which compared favorably with grating-based resonators. The main disadvantage of this device is its multiresonant response. To overcome this drawback, the authors suggested the use of k-selective transducers or the use of cascaded devices with offset resonances.

V. Straight-Edge MSW Resonators

A. Theory of Operation

The straight-edge resonator (SER), shown in Fig. 11, consists of a ferrimagnetic resonant cavity placed on a thin-film transducer structure. The resonant cavity is made of a piece of GGG/YIG cut into a rectangle by a wafer saw. Short-circuited microstrip transducers are used to couple energy in and out of the resonator. Depending on the orientation of the bias magnetic field with respect to the wave propagation direction, both MSSW-SER's and MSFVW-SER's can be constructed [15]–[17].

In the case of the MSSW-SER, in which the bias field is in the plane of the YIG film and perpendicular to the propagation direction, these waves propagate along the surface of the YIG film and are reflected onto the other surface at the straight edges. A standing wave pattern results if the following condition is met:

$$(k^{+}_{n,m} + k^{-}_{n,m})l = 2n\pi \tag{21}$$

where the wavenumbers inside the YIG film are given by

$$k^{\pm 2}_{n,m} = k^{\pm 2}_{n} + \left(\frac{m\pi}{W\Omega_1}\right)^2, \quad (n = 1,2,3,4,\cdots), (m = 1,2,3,4,\cdots) \tag{22}$$

and outside the YIG film they are given by

$$k^{\pm 2}_{n,m} = k^{\pm 2}_{n} + \left(\frac{m\pi}{W}\right)^2 \tag{23}$$

where

$$\Omega_1 = 1 - \frac{\omega \cdot \omega_M}{\omega^2 - \omega_M^2}. \tag{24}$$

From the above equations, the frequency response of the resonator, which is a family of resonant modes corresponding to different values of n and m, can be solved for a given bias magnetic field. The frequency variation of $(k^{+}_{n,m} + k^{-}_{n,m})$ is shown in Fig. 12.

In the case of the MSFVW-SER, in which the bias field is perpendicular to the YIG film, the magnetostatic waves propagate in the volume of the YIG film and are reflected by the straight edges of the film. Since the MSFVW's are isotropic waves, a standing wave pattern results in the rectangle cavity if the following condition is met:

$$k_{n,m} l = n\pi, \qquad n, m = 1,2,3,\cdots \tag{25}$$

where $k_{n,m}$ are the width mode wavenumbers of the MSFVW's. The frequency variation of $k_{n,m}$ is shown in Fig. 13.

B. Two-Port MSSW Straight-Edge Resonators

The frequency response of the MSSW-SER with a given dimension of l and W is a family of resonant modes

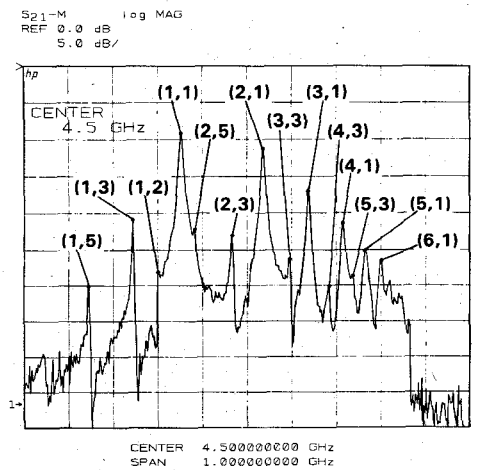

Fig. 14. Frequency response of MSSW-SER's showing the width modes (after Chang *et al.* [16]).

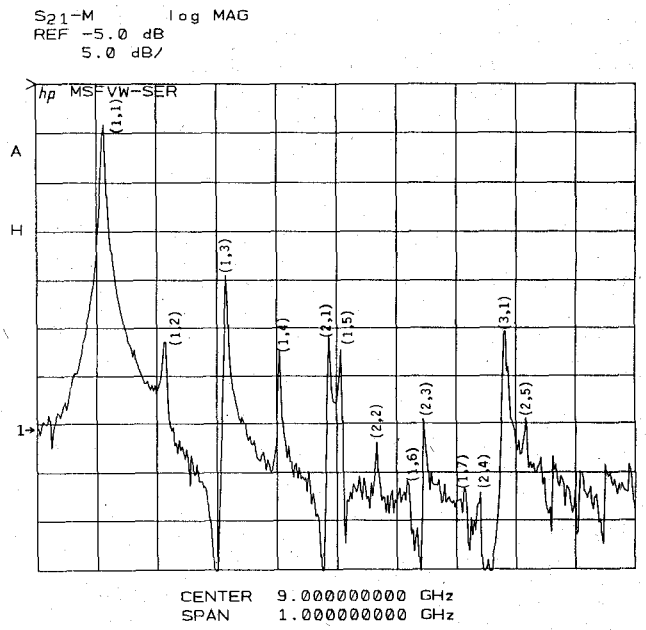

Fig. 15. Frequency response of MSFVW-SER's showing width modes at the high-frequency end (after Chang *et al.* [17]).

corresponding to different values of n and m. Depending on the current distribution on the short-circuited microstrip transducer, both odd symmetry ($m = 3,5,7,\cdots$) and even symmetry ($m = 2,4,6,\cdots$) width mode resonances can be excited by the input microwave signal. From the dispersion curves for MSSW width modes (Fig. 12), one can see that the high-order width mode resonances ((1,2), (1,3),(1,4),$\cdots$; and (2,2),(2,3),$\cdots$; (3,2),(3,3),$\cdots$;) occur at frequencies below the principal resonances ((1,1); (2,1);(3,1);$\cdots$). The symbols (n,m) are used for the classification of these resonances, as shown in Fig. 14. In this particular experiment, only the odd-order width mode resonances were strongly excited, because the current distribution on the short-circuited transducer was almost uniform ($\lambda_{em}/4 \gg L_{\text{trans}}$) over the coupling length L_{trans} that is the same as the width W of the rectangular YIG film.

Another important characteristic of MSSW's is the reduction of the available bandwidth as a function of the tuning frequency (or external bias field). This causes the high-order width modes (for example: (2,5);(3,7),(3,5);(4,9),(4,7);$\cdots$) of the high-order principal resonance to cross over and interfere with the main resonance (1,1). In the case where this width mode resonance is strongly excited, the interference may result in splitting of the main resonant peak. On the other hand, when the width mode resonance is weakly excited, this crossover of high-order width mode resonance will only cause a reduction of the loaded Q of the main resonance at the crossover frequency.

C. Two-Port MSFVW Straight-Edge Resonators

The frequency response of the MSFVW-SER with a given dimension of l and W is a family of resonant modes (n,m) similar to that of the MSSW-SER. However, the high-order width mode resonances ($m = 2,3,4,\cdots$) for the MSFVW-SER occur at the high-frequency side of the main resonances, as shown in Fig. 15 [17]. Because of this difference and the difference between the tuning characteristic of MSSW's and MSFVW's, the high-order width mode resonances for MSFVW-SER do not interfere with the main (1,1) as the resonator is tuned. Fig. 15 also shows that both the odd- and the even-order width mode resonances are excited. However, the odd-order width mode resonances are stronger than even-order width mode resonances because of the nonuniform ($\lambda_{em}/4 \approx L_{\text{trans}}$) current distribution over the coupling length of the microstrip transducers.

D. Design Parameters for Two-Port SER's

The important design parameters and performance criteria of the two-port MSW-SER will be discussed in the next section. These parameters can be divided into geometrical and material parameters:

Geometrical parameters: $\boldsymbol{H}$, l, W, L_{trans}, s, and a
Material parameters: $4\pi M_s$, ΔH, and d.

In the following section, the effect of each of the above parameters on the frequency response on the SER will be discussed.

Parameter $\boldsymbol{H}$: The orientation of the bias magnetic field determines the mode of MSW propagation. As discussed earlier, it is advantageous to use MSFVW for ease of magnet design, high-power operation, and, more importantly, to avoid width mode interference.

Parameter l: From the resonant conditions of MSSW-SER's and MSFVW-SER's, one can see that the parameter l determines the magnetostatic wavelength ($l = \lambda_{1,1}/2$) of the propagating wave. Moreover, it was shown above that the separation between the main resonance and the width modes is inversely proportional to $\lambda_{1,1}$. This implies that to reduce the interference of width modes with the main resonance and, hence, to obtain a better frequency response, the parameter l should be as small as possible. On the other hand, reducing l also reduces the power required

TABLE I
LINEWIDTHS OF YIG FILMS

Sample	$d(\mu m)$	$\Delta H_K(Oe)$ at $3GHz$	$\Delta H_K(Oe)$ at $4GHz$	$\Delta H_K(Oe)$ at $9GHz$
Airtron	79		0 85	1.8
Airtron	52	..	1.10	1.7
Airtron	120		1 25	2 5
Hitachi	20	0 36	0 45	0.71
Hitachi	23	0.45	0.63	0.89
Hitachi	21	0.45	0.54	0 80
Crismatec	20		0 63	0 85
Crismatec	30	..	0 70	1.10
Allied	25		1 10	1 40
Allied	28		0 70	1 10
Allied	100	3 0	4 46	7 14

to saturate the resonator because of the reduction of the volume of the YIG film. This suggests that there exists an optimum value of l that results in good off-resonance suppression and good power handling.

Parameter W: This parameter determines the wavelength of the width mode resonances. From the width mode dispersion relation calculations, one can see that reducing the value of W will increase the frequency separation between the width mode resonances and result in better rejection of the (1,2) resonance with respect to the main resonance (1,1) at high tuning frequencies, where the current distribution on the short-circuited microstrip is no longer constant. It was also found [16] that the ratio W/l is important in determining the strength of the width mode interference. Similar remarks apply to W regarding power saturation. As W decreases, the volume of the device decreases and hence its power-handling capability decreases.

Parameter L_{trans}: This parameter determines the reference plane of the input and output reflection coefficients. The current distribution on the transducers, overlapped with the width W of the SER, determines the excitation of odd or even width mode resonances of the MSW-SER.

Parameter s: The input and output impedance of the resonator at the main resonance (1,1) can be adjusted by adjusting s. Therefore, s determines the mismatch loss and, accordingly, the total insertion loss of the resonator.

Parameter a: Increasing the value of a will reduce the coupling efficiency to the high-order principal resonances and improve the spurious rejection of these resonances with respect to the main resonance.

Parameter d: Because the power compression level of the resonator is proportional to its volume, for a given dimension of l and W, the thicker the film the better the power-handling ability of the SER.

Parameter ΔH_K: For a given dimension of the MSW-SER, the smaller the value of ΔH_K, the stronger the coupling between the microwave current in the microstrip transducers and the spin system in the YIG film. Therefore, lower ΔH_K results in lower resonator losses. On the other hand, it will be shown later that the phase noise performance of the device degrades as ΔH_K decreases.

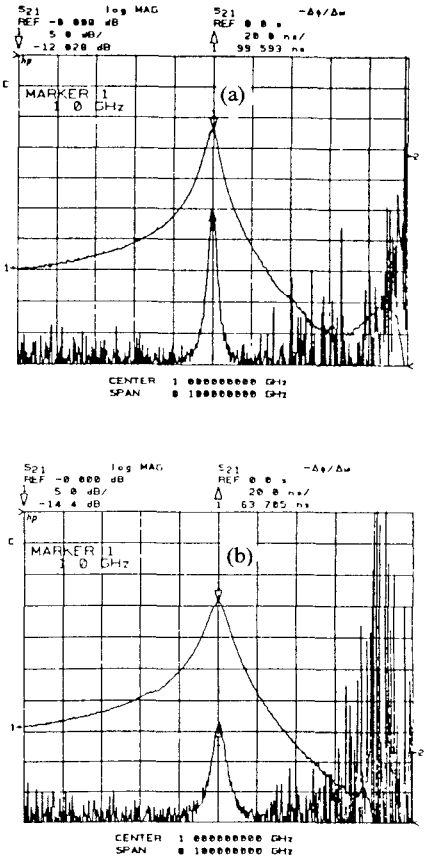

Fig. 16. Frequency response (upper trace) and group delay (lower trace) of MSFVW-SER's using (a) low ΔH_K and (b) high ΔH_K YIG films [17].

Table I shows the values of ΔH_K for a number of YIG films from different vendors. These values were measured using one-port reflection experiments with the HP-8510A Microwave Network Analyzer.

Parameter $4\pi M_s$: One can improve the power handling of MSSW-SER's below 4.2 GHz by using doped YIG films with lower $4\pi M_s$.

E. Power Handling and Phase Noise Characteristics of SER's

In addition to the volume of the MSW resonator, two other major factors affect its power-handling capability. They are the coincidence-limiting and the ferrite-limiting effects. The coincidence-limiting effect is related to a subsidiary absorption phenomenon resulting from coupling between the uniform precession mode and the spin waves of half the frequency of the uniform mode [1]. At frequencies where this effect occurs, the MSW devices saturate at a particularly low power level (typically $\leqslant -10$ dBm). For MSSW devices, this phenomenon can occur at frequencies below ω_M depending on the bias field value, and will always occur for frequencies below $2\omega_M/3$. In the case of MSFVW devices, unless the magnetostatic wavelength is very small ($\leqslant$ few micrometers), coincidence limiting is not encountered. For pure YIG films, $4\pi M_s$ is about 1760 G, which means that MSSW resonators may suffer from coincidence-limiting effects for frequencies below 4.9 GHz.

TABLE II
EFFECT OF YIG LINEWIDTH OF THE RESONATOR PERFORMANCE

Parameter	$\Delta H = 0.75Oe$	$\Delta H = 1.6Oe$
I.L. (dB)	−12.0	−14.4
Q_{loaded}	300	200
1dB compression(dBm)	−10	+6

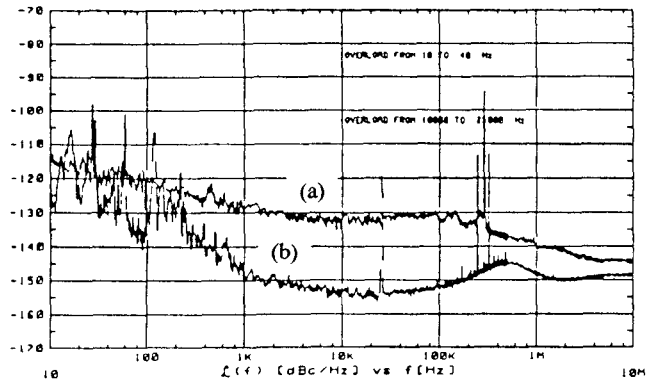

Fig. 17. Phase noise characteristics of SER's using (a) low ΔH_K and (b) high ΔH_K YIG films (after Chang *et al.* [23]).

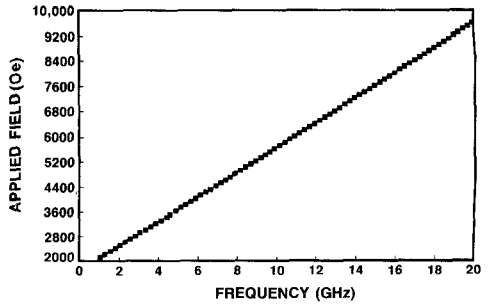

(a)

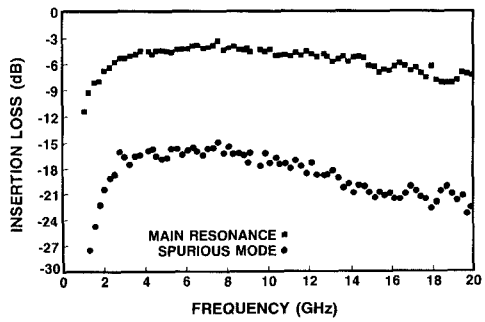

(b)

Fig. 18. (a) Tuning characteristics and (b) insertion loss characteristics of MSFVW-SER's (after Chang *et al.* [17]).

The second power-limiting mechanism, the premature saturation of the main resonance, is common to all ferrite devices and occurs at all frequencies and is a function of the ferrite linewidth ΔH and the spinwave linewidth ΔH_K. It is this effect that sets the limit on the power-handling capability of the MSW-SER.

Several MSFVW-SER's were fabricated using YIG films with different ΔH_K to examine the power-handling effects. Fig. 16(a) and (b) shows the insertion loss of two such devices using two films with ΔH_k of 0.75 Oe and 1.6 Oe, respectively. The lower trace in each figure is a plot of the group delay of the resonator from which the loaded Q of the device can be estimated ($Q_{\text{loaded}} = \omega\tau/2$). Table II shows the insertion loss, loaded Q, and the 1-dB power compression levels for the two devices. In spite of the small difference in the insertion loss (about 2 dB), the power-handling capabilities of the two devices were quite different, varying by more than 15 dB.

The phase noise characteristics of MSW-SER's were measured using an HP-3047A Spectrum Analyzer System and the results were published elsewhere [17]. In one particular experiment, the phase noise characteristics were measured for the devices mentioned in Table II, using input power values below the 1-dB compression levels to avoid saturation effects. Fig. 17 shows the data obtained from such measurement. Both devices exhibited a $1/f$ noise spectral density behavior at low-frequency offsets. This was not surprising because similar results were noticed for other physical wave devices such as surface acoustic wave (SAW) resonators and delay lines. Moreover, the device built using a high ΔH_K YIG film exhibited a 20-dB lower noise floor than the low ΔH_K device. In a previous paper, a simple theory was given to explain such behavior [23]. It was pointed out that low values of ΔH result in more spontaneous transitions of spins from high-energy states to low-energy states. During spontaneous transitions, the spins emit quanta of energy which correspond to the resonance, and bear random phase relation to each other and the total radiation field. This process is responsible for the high level of noise floor observed in Fig. 17.

F. Tuning Characteristics of Two-Port SER's

Several SER's were fabricated and tested using MSSW's and MSFVW's with various YIG film thicknesses and geometries. In the case of MSSW-SER's, the parameter l was varied from 200 to 2000 μm and the parameter W was varied from 2 to 5 mm. It was found that the lowest insertion loss together with the highest off-resonance rejection was obtained when $l \approx 400$ μm, $s = 100$ μm, and $W = 2.5$ mm. The resonator was tuned from 2 to 16 GHz with coincidence limiting reducing the 1-dB power compression level to below -20 dBm for frequencies below 4.5 GHz. Above 4.5 GHz, the resonator did not show premature saturation effects up to a power level of +5 dBm [16].

The MSFVW-SER was optimized for off-resonance suppression and power handling over the 1–22-GHz frequency range [17]. Using thick YIG films ($t \geq 75$ μm) with $\Delta H_K \geq 1$ Oe at X-band, the tuning characteristics of the devices were as shown in Fig. 18(a) and (b). A typical frequency response (S_{12}) of such resonator is shown in Fig. 19(a), (b), and (c) at 5, 15, and 20 GHz, respectively. In each of these figures, the corresponding reflection response (S_{11}) is shown plotted in Smith chart format. The 1-dB power compression level for this resonator was above +5 dBm for most of the tuning range. These impressive characteris-

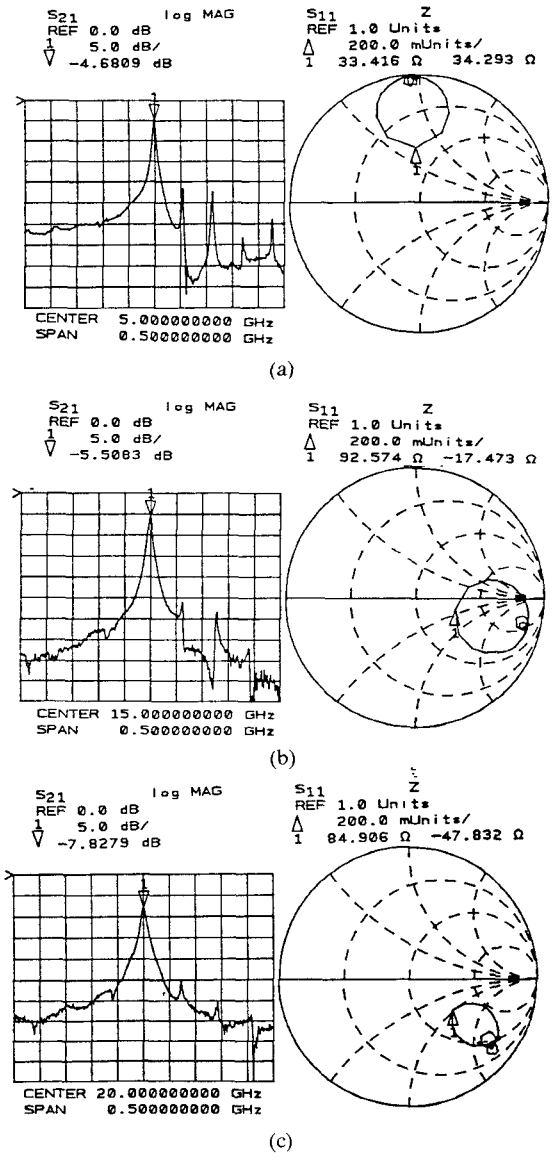

Fig. 19. Typical frequency responses for the MSFVW-SER at (a) 5 GHz, (b) 15 GHz, and (c) 20 GHz (after Chang *et al.* [17]).

tics compare very favorably with competing technologies such as YIG sphere resonators with the added advantages of simplicity of fabrication and integration with MMIC subsystems.

G. One-Port MSW Straight-Edge Resonators

Kunz *et al.* [24] designed one-port SER's using MSSW's and MSFVW's. These devices provide frequency-selective elements with very high Q for tunable oscillator applications [25]. Several schemes were used, including side coupling and top coupling between the YIG film and the microstrip transducer. The side-coupled one-port resonator was exactly the same as the two-port device without one of the microstrip transducers. In the top-coupling scheme, a microstrip transducer was centered on top of the YIG film. Several microstrip widths, YIG film widths, and spacers (between the transducer and the YIG film) were used to achieve a variety of coupling coefficients. The device was integrated with microwave transistors to make microwave tunable reflection oscillators in which the negative resistance of the transistor was matched with an equal resonator radiation resistance. A complete description of the one-port resonators together with oscillator applications will be included in a later paper [25].

VI. Conclusions

Magnetostatic wave resonators have been investigated for applications in the microwave frequency ranges. Grating-based resonators using MSSW's and MSFVW's promise high Q but require large YIG film dimensions and, hence, large magnet sizes as well as nontrivial processing steps. Metal gratings can be used as reflectors, yielding simple device fabrication. However, the insertion losses of metal-based gratings are higher than those of etched-groove gratings. Ring resonators have been demonstrated at S-band but they require more research to eliminate the multimode response inherent in the circulating wave scheme.

Straight-edge resonators using rectangular pieces of YIG films were reviewed in detail. They are simple structures which can be easily integrated with MMIC subsystems for tunable oscillator, preselector, and frequency multiplier applications. The MSFVW-SER two-port resonators were tunable from 1 to 22 GHz with insertion losses of about 6 dB over most of the tuning range. Carefully choosing the resonator physical and material parameters resulted in better than 10 dB of off-resonance suppression and a loaded Q of more than 1000. The Q increased to 2000 at the high-frequency end. The device is small, permits compact magnet designs, and does not require critical processing steps.

Acknowledgment

The authors would like to thank B. Kunz, E. Reese, and H. Tanbakushi for useful discussions. They would also like to thank E. Luiz, who assembled the devices. We are also grateful to W. Shreve for his critical review of the manuscript.

References

[1] J. P. Parekh, Ed., *Special Issue of Trans. Circuits, Syst., Signal Process*, vol. 4, no. 1–2, 1985.
[2] W. S. Ishak and K. W. Chang, "Magnetostatic wave devices for microwave signal processing," *Hewlett-Packard J.*, vol. 36, no. 2, pp. 10–20, Feb. 1985.
[3] W. S. Ishak, "Microwave signal processing using magnetostatic wave devices," in *Proc. IEEE Ultrasonics Symp.*, 1984, pp. 152–163.
[4] J. M. Owens, R. L. Carter, C. V. Smith, Jr., and J. H. Collins, "Magnetostatic waves, microwave SAW?," in *Proc. IEEE Ultrasonics Symp.*, 1980, pp. 506–513.
[5] C. G. Sykes, J. D. Adam, and J. H. Collins, "Magnetostatic wave propagation in a periodic structure," *Appl. Phys. Lett.*, vol. 29, no. 6, pp. 388–391, Sept. 1976.
[6] J. P. Parekh and H. S. Tuan, "Reflection of magnetostatic forward volume waves by a shallow-grooved grating on a YIG film," *IEEE Trans. Microwave Theory Tech.*, vol. MTT-26, pp. 1039–1044, Dec. 1978
[7] J. H. Collins, J. D. Adam, and Z. M. Bardai, "One-port magnetostatic wave resonator," *Proc. IEEE*, vol. 65, pp. 1090–1092, July 1977

[8] J. M. Owens, C. V. Smith, Jr., E. P. Snapka, and J. H. Collins, "Two-port magnetostatic wave resonators utilizing periodic reflective arrays," in *Proc. IEEE Ultrasonics Symp.*, 1978, pp. 440–442.
[9] J. P. Castera, "Magnetostatic volume wave resonators," in *Proc. IEEE-MTT Symp.*, 1979, pp. 157–159.
[10] W. R. Brinlee, J. M. Owens, C. V. Smith, Jr., and R. L. Carter, "Two-port magnetostatic wave resonators utilizing periodic metal reflective arrays," *J. Appl. Phys.*, vol. 52, no. 3, pp. 2276–2278, Mar. 1981.
[11] J. P. Castera, "New configurations for magnetostatic wave devices," in *Proc. IEEE Ultrasonics Symp.*, 1980, pp. 514–517.
[12] J. P. Castera and P. Hartmann, "A multipole magnetostatic wave resonator filter," *IEEE Trans. Magn.*, vol. MAG-18, no. 6, pp. 1601–1603, 1982.
[13] T. D. Poston and D. D. Stancil, "A new microwave ring resonator using guided magnetostatic surface waves," *J. Appl. Phys.*, vol. 53, no. 6, Mar. 1984.
[14] E. Huijer and W. S. Ishak, "MSSW resonators with straight-edge reflectors," *IEEE Trans. Magn.*, vol. MAG-20, pp. 1232–1234, Sept. 1984.
[15] E. Huijer, U.S. Patent 4 528 529, 1985.
[16] Kok-Wai Chang and W. S. Ishak, "Magnetostatic surface wave straight-edge resonators," *Trans. Circuits, Syst., Signal Proc.*, vol. 4, no. 1–2, pp. 201–209, 1985.
[17] ——, "Magnetostatic forward volume wave straight-edge resonators," in *Proc. IEEE-MTT Symp.*, 1986, pp. 473–475.
[18] R. W. Damon and J. R. Eshbach, "Magnetostatic modes of a ferromagnetic slab," *J. Phys. Chem. Solids*, vol. 19, pp 308–320, 1961.
[19] M. R. Daniel, J. D. Adam, and T. W. O'Keeffe, "Linearly dispersive delay lines at microwave frequencies using magnetostatic waves," in *Proc. IEEE Ultrasonics Symp.*, 1979, pp. 806–809.
[20] J. D. Adam, "A temperature stabilized magnetostatic wave device," in *Proc. IEEE-MTT Symp.*, 1979, pp. 160–161.
[21] H. Tanbakushi, private communications.
[22] E. Reese, Jr., private communications.
[23] Kok-Wai Chang and W. S. Ishak, "Phase noise characteristics of MSW devices," in *Proc. IEEE Ultrasonics Symp.*, 1985, 163–168.
[24] W. Kunz, Kok-Wai Chang, and W. S. Ishak, "Magnetostatic wave resonators," Patent filed, 1986.
[25] W. Kunz, Kok-Wai Chang, and W. S. Ishak, "Tunable oscillators using magnetostatic wave resonators," presented at 1986 Ultrasonics Symp.

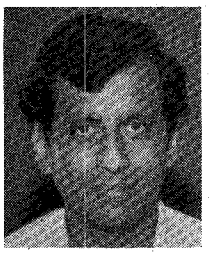

Waguih S. Ishak (S'73–M'78) was born in Cairo, Egypt, on December 4, 1949. He received the B.Sc. degree in electrical engineering and the B.Sc. degree in mathematics from Cairo University and Ain-Shams University in 1971 and 1973, respectively.

He worked as a teaching assistant with the Department of Mathematics and Physics at Cairo University from 1971 to 1973. He obtained the M.Sc. degree in 1974 and the Ph.D. degree in 1978 both in electrical engineering from McMaster University, Hamilton, Ontario, Canada. He received a post-doctoral Fellowship from the National Research Council of Canada in 1978 where he did research on modeling of magnetic bubble devices.

He was a teaching fellow with the Department of Material Research, American University in Cairo in 1972. In 1978, he joined the Physical Research Laboratory at Hewlett-Packard Laboratories, Palo Alto, CA, to work with the bubble memory group where he spent a year on bubble propagation and detection circuit testing. He became a project leader in 1982 and, in 1984, he became a project manager of the sources and signal processing group. His current research interests involve surface acoustic wave devices, magnetostatic wave devices, and multilayer semiconductor structures. He wrote more than 25 technical papers in the area of bubble memories, numerical optimization, surface acoustic wave devices, and magnetostatic wave devices.

Kok-Wai Chang (M'86) was born in Hong Kong. He studied physics at National Chung King University, from which he earned a B.Sc. degree in 1977. He continued his studies at Cambridge University and Texas Christian University, and he received the Ph.D. degree in 1982.

He worked as a research associate at the University of Texas at Arlington from 1982 to 1984 and then he joined Hewlett-Packard Laboratories to work on magnetostatic wave device modeling. His current research interests involve magnetic devices, microwave devices, and magnetooptical applications. He wrote several papers in the area of molecular spectroscopy and magnetostatic wave devices.